

Anomalous Josephson effect between d-wave superconductors through a two-dimensional electron gas with both Rashba spin-orbit coupling and Zeeman splitting

Bin-Hao Du(杜彬豪), Mou Yang(杨谋), and Liang-Bin Hu(胡梁宾)
Citation: Chin. Phys. B, 2023, 32 (**7**): 077201. DOI: 10.1088/1674-1056/accc7f
Journal homepage: http://cpb.iphy.ac.cn; http://iopscience.iop.org/cpb

What follows is a list of articles you may be interested in

---

nfluence of Rashba spin-orbit coupling on Josephson effect in triplet superconductor/two-dimensional semiconductor/triplet superconductor junctions

Bin-Hao Du(杜彬豪), Man-Ni Chen(陈嫚妮), and Liang-Bin Hu(胡梁宾)
Chin. Phys. B, 2022, 31 (**7**): 077201. DOI: 10.1088/1674-1056/ac587e

Influence of spin-orbit coupling on spin-polarized electronic transport in magnetic semiconductor nanowires with nanosized sharp domain walls

Lian Liu(刘恋), Wen-Xiang Chen(陈文祥), Rui-Qiang Wang(王瑞强), Liang-Bin Hu(胡梁宾)
Chin. Phys. B, 2018, 27 (**4**): 047201. DOI: 10.1088/1674-1056/27/4/047201

Spin transport in a chain of polygonal quantum rings with Dresselhaus spin-orbit coupling

Han-Zhao Tang(唐翰昭), Xiao-Teng Yao(要晓腾), Jian-Jun Liu(刘建军)
Chin. Phys. B, 2017, 26 (**11**): 117203. DOI: 10.1088/1674-1056/26/11/117203

Spin-polarized current in double quantum dots

Li Ai-Xian (李爱仙), Duan Su-Qing (段素青)
Chin. Phys. B, 2012, 21 (**11**): 117201. DOI: 10.1088/1674-1056/21/11/117201

Thermospin effects in parallel coupled double quantum dots in the presence of the Rashba spin–orbit interaction and Zeeman splitting

Xue Hui-Jie(薛惠杰), LŰ Tian-Quan(吕天全), Zhang Hong-Chen(张红晨), Yin Hai-Tao(尹海涛), Cui Lian(催莲), and He Ze-Long(贺泽龙)
Chin. Phys. B, 2012, 21 (**3**): 037201. DOI: 10.1088/1674-1056/21/3/037201

Anomalous Josephson effect between d-wave superconductors through a two-dimensional electron gas with both Rashba spin–orbit coupling and Zeeman splitting

Bin-Hao Du(杜彬豪), Mou Yang(杨谋), and Liang-Bin Hu(胡梁宾)†

Guangdong Provincial Key Laboratory of Quantum Engineering and Quantum Materials, School of Physics and Telecommunication Engineering, South China Normal University, Guangzhou 510631, *China*

(Received 18 October 2022; revised manuscript received 17 March 2023; accepted manuscript online 13 April 2023)

Based on the Bogoliubov–de Gennes equation and the extended McMillan's Green's function formalism, we study theoretically the Josephson effect between two d-wave superconductors bridged by a ballistic two-dimensional electron gas with both Rashba spin–orbit coupling and Zeeman splitting. We show that due to the interplay of Rashba spin–orbit coupling and Zeeman splitting and d-wave pairing, the current–phase relation in such a heterostructure may exhibit a series of novel features and can change significantly as some relevant parameters are tuned. In particular, anomalous Josephson current may occur at zero phase bias under various different situations if both time reversal symmetry and inversion symmetry of the system are simultaneously broken, which can be realized by tuning some relevant parameters of the system, including the relative orientations and the strengths of the Zeeman field and the spin–orbit field in the bridge region, the relative orientations of the *a* axes in two superconductor leads, or the relative orientations between the Zeeman field in the bridge region and the *a* axes in the superconductor leads. We show that both the magnitude and the direction of the anomalous Josephson current may depend sensitively on these relevant parameters.

Keywords: anomalous Josephson effect, d-wave pairing, Rashba spin–orbit coupling, Zeeman splitting

PACS: 72.25.Dc, 72.25.Ba, 74.78.Na, 85.25.Cp **DOI:** 10.1088/1674-1056/accc7f

1. Introduction

The Josephson effect in hybrid mesoscopic systems involving conventional or unconventional superconductors have been extensively studied for decades.[1–5] Such hybrid mesoscopic systems provide ideal platforms for studying various aspects of the superconducting proximity effect. For example, in a conventional superconductor/topological insulator/conventional superconductor junction, the proximity effect between the superconducting paring and the helical spin–momentum locking of the topological insulator surface states may lead to the formation of Majorana zero modes[6] and odd-frequency pairing,[7] which have been viewed as rarely occurring in nature. The Josephson effect in various types of hybrid mesoscopic systems is not only of theoretical interest but also of practical importance, which are the key elements of superconducting electronics and also the bases of some conceptually new types of superconducting electronic components proposed in recent years, such as superconducting qubits,[8] cryogenic memories,[9] superconducting phase batteries,[10] phase qubits,[11] rectifiers,[12] *etc*.

The dissipationless Josephson current I_J flowing in a Josephson junction is related to the macroscopic phase difference ϕ of the superconducting order parameters between two superconductor leads. This relation is described by the current–phase relationship (CPR). The CPR is an important characteristic of a Josephson junction and its features link with the symmetries of the junction. For instance, in the presence of time-reversal symmetry or inversion symmetry, the constraint $I_J(\phi) = -I_J(-\phi)$ is satisfied, which results in the vanishing of the Josephson current at $\phi = 0$. If both time-reversal symmetry and inversion symmetry are preserved, the CPR in its simplest form, reads $I_J(\phi) = I_C \sin(\phi)$, with I_C the critical current. Such a Josephson junction is called a 0-junction, the Josephson free energy of which is minimum at $\phi = 0$. However, if time-reversal symmetry or inversion symmetry is broken in a Josephson junction, the junction can turn into a π-junction, the Josephson free energy of which is minimum at $\phi = \pi$ but not at $\phi = 0$. In a π-junction, the direction of the flow of the Josephson current at a phase bias ϕ is reversed as compared with that in a 0-junction at the same phase bias. It is predicted that π-junctions and controllable 0–π transitions may find some important applications in superconducting electronics, such as in the design of noise-immune superconducting qubits[8] and cryogenic memory.[9] The 0–π transitions in conventional superconductor/ferromagnet/conventional superconductor junctions have been intensively studied in the past decades, which may result from Zeeman splitting by exchange interaction in the ferromagnetic layers sandwiched between two conventional s-wave superconductors. If a single ferromagnetic layer is sandwiched between two superconductor leads, the 0–π transition can be induced by tuning the thickness of the ferromagnetic layer.[13] If multiple

†Corresponding author. E-mail: lbhu26@126.com

© 2023 Chinese Physical Society and IOP Publishing Ltd

ferromagnetic layers are sandwiched between two superconductor leads, the 0–π transition can also be induced by tuning the relative orientations of the magnetizations in different ferromagnetic layers.[14] In some recent studies, it was also found that when two conventional s-wave superconductors are linked by a bridge with strong intrinsic spin–orbit coupling (SOC), which may originate from either bulk inversion asymmetry (such as Dresselhaus SOC[15]) or structural inversion asymmetry (such as Rashba SOC[16]), the 0–π transition can also be induced by tuning the strength of SOC in the bridge region.[2] Moreover, when strong SOC is in appropriate combination with Zeeman splitting in the bridge region, an anomalous phase shift may be induced in the Josephson current, which can take an intermediate value ϕ_0 between 0 and π. Such a Josephson junction is called a ϕ_0-junction, the minimum of the Josephson free energy of which occurs at the phase bias $\phi = \phi_0$ but not at $\phi = 0$ or at $\phi = \pi$. The presence of this anomalous phase shift implies that the Josephson current can flow between two superconductor leads even at zero phase bias. Such phenomenon is called the anomalous Josephson effect. Experimentally, the anomalous Josephson effect has recently been observed in Josephson junctions through a quantum dot[17] and Bi_2Se_3 interlayer.[4] It is predicted that the anomalous Josephson effect may also find some important applications in superconducting electronics, such as superconducting phase batteries,[10] phase qubits,[11] and rectifiers,[12] *etc*. Due to these possibilities, various different ways have been proposed in recent years focusing on breaking both the time-reversal and the parity symmetries of a Josephson junction to create anomalous Josephson current at zero phase bias.

From the theoretical points of view, the anomalous Josephson effect is relate to the inverse Edelstein effect observed in some normal metals or semiconductors with strong SOC. While the Edelstein effect consists in the generation of an out-of-equilibrium spin polarization by a charge current,[18–21] the inverse Edelstein effect, also called the spin-galvanic effect, consists in the generation of a charge current by an out-of-equilibrium spin polarization.[22–24] Both these two kinds of magnetoelectronic effects have been observed experimentally in some normal metals and semiconductors with strong SOC.[19–21,23,24] From the theoretical points of view, if in a Josephson junction two superconductor leads are linked by a bridge with strong SOC, similar magnetoelectronic effects may also occur in the junction, and in particular, if Zeeman splitting coexists with strong SOC in the bridge region, a finite Josephson current may also be generated in the junction even at zero phase bias due to the occurrence of out-of-equilibrium spin polarization in the bridge region, similar to the spin-galvanic effect found in some normal metals or semiconductors with strong SOC. Due to this similarity, the anomalous Josephson effect in such types of Josephson junctions may also be viewed as a kind of spin-galvanic effect.[1,25,26]

In this paper we study theoretically the Josephson effect in a ballistic Josephson junction in which two d-wave superconductor leads are linked by a bridge of two-dimensional electron gas (2DEG) with both Rashba SOC and Zeeman splitting. Up to now, while the features of the Josephson effect in junctions consisting of conventional superconductor leads and various types of bridges with strong SOC and Zeeman splitting have been intensively studied in recent years,[27–37] what peculiar features the Josephson effect may exhibit in junctions consisting of unconventional superconductor leads linked by bridges with both strong SOC and Zeeman splitting remains to be further investigated in some detail. From the theoretical points of view, since pairing potentials in unconventional superconductors are anisotropic and depend on the directions of quasi-particles' motions, the interplay of strong SOC and Zeeman splitting on the Josephson effect in junctions consisting of unconventional superconductor leads may be more subtle as compared with that in junctions consisting of conventional s-wave superconductor leads. For instance, in the d-wave case, the influence of SOC and Zeeman splitting on the propagations of quasi-particles may depend not only on the relative orientations and the relative strengths of the spin–orbit field and the Zeeman field in the bridge region but also depend on the relative orientations between the a axes in two d-wave superconductor leads,[38] and due to such complicated dependences, it is possible that more rich features may be exhibited in the Josephson effect in such junctions. In this paper we take such complicated orientation dependences into account and present a systematical theoretical investigation on the features of the Josephson effect between two d-wave superconductor leads linked by a bridge of 2DEG with the simultaneous presence of both Rashba SOC and Zeeman splitting. Our studies are based on the McMillan's Green's function formalism,[39] which is a suitable formalism for studying quasi-particle transport in ballistic superconducting junctions.[39–41] We extend this formalism to include the interplay of Rashba SOC and Zeeman splitting and d-wave pairing, and based on the extended formalism, we calculate the Josephson current and the current–phase relation under various different situations. We show that due to the coexistence of multiple complicated factors, the interplay of Rashba SOC and Zeeman splitting on the Josephson effect in such heterostructures may exhibit a series of novel features, and in particular, we show that anomalous Josephson current may occur at zero phase bias under various different situations in such a junction, which depends sensitively not only on the strengths of Rashba SOC and Zeeman splitting but also on the relative orientations of the Zeeman field in the bridge region and the relative orientations of the a axes in two d-wave superconductor leads.

The paper is organized as follows. In Section 2 we

present the model Hamiltonian and construct the McMillan's Green's function formalism for calculating the Josephson current and the current-phase relation. The numerical results for the Josephson current and the current-induced relation are presented and discussed in Section 3. Finally, a summary is given in Section 4.

2. Model and formulation

We consider a ballistic Josephson junction in which two d-wave superconductor leads are linked by a bridge of two-dimensional electron gas with both Rashba SOC and Zeeman splitting. The junction lies in the y–z plane. The two interfaces between the bridge region and the two superconductor leads extend along the y direction and are located at $z=0$ and L, respectively, with L the width of the bridge region. For simplicity, the junction interfaces are assumed to be perfectly flat and transparent. The direction of the superconducting phase bias is along the z direction. To open a gap at the crossing point of two split bands by Rashba SOC, we assume that a Zeeman field $\boldsymbol{h}=(h_x,h_y,h_z)$ is applied in the bridge region. The low-energy electron and hole excitations of the system can be described by the following Bogoliubov–de Gennes (BdG) Hamiltonian[42]

$$\hat{H}_{\rm BdG}=\begin{bmatrix}\hat{H}(\boldsymbol{k}) & \hat{\Delta}(\boldsymbol{k})\\ -\hat{\Delta}^*(-\boldsymbol{k}) & -\hat{H}^*(-\boldsymbol{k})\end{bmatrix}, \tag{1}$$

with the spinor basis $\hat{\Psi}=[\hat{\psi}_\uparrow,\hat{\psi}_\downarrow,\hat{\psi}_\uparrow^+,\hat{\psi}_\downarrow^+]^{\rm T}$ in Nambu-spin space, where the arrow index $(\uparrow,\downarrow)$ corresponds to real spin. The single-particle Hamiltonian $\hat{H}(\boldsymbol{k})$ is given by

$$\hat{H}(\boldsymbol{k})=[\xi_{\boldsymbol{k}}-\mu]\sigma_0+\Theta(z)\Theta(L-z)[\boldsymbol{h}\cdot\sigma+\alpha_{\rm R}(k_z\sigma_y-k_y\sigma_z)], \tag{2}$$

where $\xi_{\boldsymbol{k}}=\hbar^2\boldsymbol{k}^2/2m$ is the kinetic energy of an electron with wave vector $\boldsymbol{k}=(0,k_y,k_z)$ and effective mass m, μ is the chemical potential, $\sigma=(\sigma_x,\sigma_y,\sigma_z)$ represent the Pauli matrices acting on the real-spin degrees of freedom, σ_0 stands for the 2×2 identity matrix, $\Theta(z)$ is the Heaviside step function, and $\alpha_{\rm R}$ is strength of Rashba SOC in the bridge region. The gap matrix $\hat{\Delta}(\boldsymbol{k})={\rm i}\Delta(\theta)\sigma_y$ is a 2×2 matrix in spin space, with the magnitude of the pairing potential given by

$$\begin{aligned}\Delta(\boldsymbol{\theta})=\Delta(T)[&\cos(2(\theta-a_{\rm L}))\Theta(-z)\\&+\cos(2(\theta-a_{\rm R}))\,{\rm e}^{{\rm i}\phi}\Theta(z-L)],\end{aligned} \tag{3}$$

where $\theta=\arccos(k_z/\boldsymbol{k})$ is the propagating angle of quasi-particles with respect to the z axis, $a_{\rm L}$ and $a_{\rm R}$ denote the angles between the z axis and the a axes in the left and the right d-wave superconductor leads, respectively, and ϕ is the macroscopic superconducting phase difference between two superconductor leads. Since only the phase difference between two superconductor leads is related to the Josephson current, for simplicity, we set the macroscopic superconducting phase equal to zero in the left superconductor lead. According to the BCS relation,[41,42] the temperature dependence of the magnitude of the pairing potential can be given by $\Delta(T)=\Delta_0\tanh(1.74\sqrt{T_{\rm c}/T-1})$, where $\Delta_0=1.76k_{\rm B}T_{\rm c}$, with $T_{\rm c}$ the critical temperature and $k_{\rm B}$ the Boltzman constant.

Since the junction is assumed to be translational invariant along the y direction, the solutions of the BdG equation can be described by the general ansatz $\psi(z)\,{\rm e}^{{\rm i}k_y y}$, where k_y is the transverse component of wave vector and $\psi(z)$ is the solution of the BdG Hamiltonian for the effective one-dimensional scattering problem along the z direction, which can be constructed from the eigensolutions of the BdG Hamiltonian in each different regions of the junction. We first solve the eigensolutions within the d-wave superconducting regions. There are eight propagating modes in these regions for a fixed quasi-particle excitation energy E and k_y. Four of them are spin-up modes, and the corresponding eigenfunctions can be written as: (i) right-going electronlike quasi-particle mode $\psi_{\rm r,e,\uparrow}=\hat{A}_1\,{\rm e}^{{\rm i}k_{\rm e}z+{\rm i}k_y y}$, (ii) right-going holelike quasi-particle mode $\psi_{\rm r,h,\uparrow}=\hat{A}_2\,{\rm e}^{-{\rm i}k_{\rm h}z+{\rm i}k_y y}$, (iii) left-going electronlike quasi-particle mode $\psi_{\rm l,e,\uparrow}=\hat{A}_3\,{\rm e}^{-{\rm i}k_{\rm e}z+{\rm i}k_y y}$, (iv) left-going holelike quasi-particle mode $\psi_{\rm l,h,\uparrow}=\hat{A}_4\,{\rm e}^{{\rm i}k_{\rm h}z+{\rm i}k_y y}$. Here the subscripts r (l), e (h), and $\uparrow$ ($\downarrow$) correspond to right (left)-going modes, electronlike (holelike) modes, and spin-up (spin-down) modes, respectively, and $\hat{A}_{i=1\sim4}$ denotes of the spinors of the corresponding quasi-particle modes. The explicit forms of the spinors $\hat{A}_{i=1\sim4}$ can be given by

$$\hat{A}_1=\begin{bmatrix}u_1e_1\\0\\0\\v_1\end{bmatrix},\ \hat{A}_2=\begin{bmatrix}v_2e_2\\0\\0\\u_2\end{bmatrix},\ \hat{A}_3=\begin{bmatrix}u_2e_2\\0\\0\\v_2\end{bmatrix},\ \hat{A}_4=\begin{bmatrix}v_1e_1\\0\\0\\u_1\end{bmatrix}, \tag{4}$$

where

$$u_{1(2)}=\sqrt{\frac{E+\Omega_{1(2)}}{2E}},\qquad v_{1(2)}=\sqrt{\frac{E-\Omega_{1(2)}}{2E}}, \tag{5}$$

$$e_1=\frac{\Delta(\theta)}{|\,\Delta(\theta)\,|},\qquad e_2=\frac{\Delta(\pi-\theta)}{|\,\Delta(\pi-\theta)\,|}, \tag{6}$$

where $\Omega_1=\sqrt{E^2-|\Delta(\theta)|^2}$ for $E>0$, $\Omega_1=-\sqrt{E^2-|\Delta(\theta)|^2}$ for $E<0$, $\Omega_2=\sqrt{E^2-|\Delta(\pi-\theta)|^2}$ for $E>0$, $\Omega_2=-\sqrt{E^2-|\Delta(\pi-\theta)|^2}$ for $E<0$. The magnitude of the z-component of the wave vectors of electronlike (holelike) quasi-particles are denoted as $k_{\rm e}$ and $k_{\rm h}$, respectively, which are related to the quasi-particle excitation energy E and the transverse component k_y of the wave vectors by the following dispersion relation: $k_{\rm E\,(H)}=\sqrt{k_{\rm e\,(h)}^2+k_y^2}=$

$\sqrt{(2m/\hbar^2)(\mu \pm \Omega)}$, where $k_{\mathrm{E\ (H)}}$ is the magnitude of the wave vector of an electronlike (holelike) quasi-particle. In general, the quasi-particle excitation energy E and the superconducting pairing potential $\hat{\Delta}(\theta)$ are both much smaller than the chemical potential μ. As a result, one can set $k_{\mathrm{E}} \approx k_{\mathrm{H}} \approx k_{\mathrm{F}}$ to simplify the theoretical treatment, where $k_{\mathrm{F}} = \sqrt{(2m\mu/\hbar^2)}$ is the magnitude of the Fermi wave vector in normal states.

Similarly, there are four spin-down propagating modes in the d-wave superconducting regions, and the corresponding eigenfunctions can be written as: i) right-going electronlike quasi-particle mode $\psi_{\mathrm{r,e},\downarrow} = \hat{B}_1 \mathrm{e}^{\mathrm{i}k_{\mathrm{e}}z+\mathrm{i}k_y y}$, ii) right-going holelike quasi-particle mode $\psi_{\mathrm{r,h},\downarrow} = \hat{B}_2 \mathrm{e}^{-\mathrm{i}k_{\mathrm{h}}z+\mathrm{i}k_y y}$, iii) left-going electronlike quasi-particle mode $\psi_{\mathrm{l,e},\downarrow} = \hat{B}_3 \mathrm{e}^{-\mathrm{i}k_{\mathrm{e}}z+\mathrm{i}k_y y}$, iv) left-going holelike quasi-particle mode $\psi_{\mathrm{l,h},\downarrow} = \hat{B}_4 \mathrm{e}^{\mathrm{i}k_{\mathrm{h}}z+\mathrm{i}k_y y}$, where the explicit forms of the spinors $\hat{B}_{i=1\sim4}$ can be given by

$$\hat{B}_1 = \begin{bmatrix} 0 \\ -u_1 e_1 \\ v_1 \\ 0 \end{bmatrix}, \quad \hat{B}_2 = \begin{bmatrix} 0 \\ -v_2 e_2 \\ u_2 \\ 0 \end{bmatrix},$$
$$\hat{B}_3 = \begin{bmatrix} 0 \\ -u_2 e_2 \\ v_2 \\ 0 \end{bmatrix}, \quad \hat{B}_4 = \begin{bmatrix} 0 \\ -v_1 e_1 \\ u_1 \\ 0 \end{bmatrix}. \tag{7}$$

In the bridge region between two superconductor leads, there are also four electron and four hole propagating modes, which can be described by the following eigenfunctions:

$$\psi_{\mathrm{e},i=1\sim4} = \begin{bmatrix} -h_x + \mathrm{i}(h_y + \alpha_{\mathrm{R}} k_{\mathrm{e},i}) \\ H_i^{\mathrm{e}} - E + h_z - \alpha_{\mathrm{R}} k_y \\ 0 \\ 0 \end{bmatrix} \mathrm{e}^{\mathrm{i}k_{\mathrm{e},i}z+\mathrm{i}k_y y},$$
$$\psi_{\mathrm{h},i=1\sim4} = \begin{bmatrix} 0 \\ 0 \\ -h_x - \mathrm{i}(h_y - \alpha_{\mathrm{R}} k_{\mathrm{h},i}) \\ H_i^{\mathrm{h}} + E + h_z + \alpha_{\mathrm{R}} k_y \end{bmatrix} \mathrm{e}^{\mathrm{i}k_{\mathrm{h},i}z+\mathrm{i}k_y y}, \tag{8}$$

where $H_i^{\mathrm{e\ (h)}} = (\hbar^2/2m)(k_{\mathrm{e\ (h)},i}^2 + k_y^2) - \mu$ and $k_{\mathrm{e\ (h)},i}$ denotes the z component of the wave vectors of electrons (holes) in the bridge region, respectively, which are related to the excitation energy E and the transverse component k_y of the wave vectors by the following dispersion relations:

$$(H_i^{\mathrm{e}} - E)^2 - h_x^2 - (h_y + \alpha k_{\mathrm{e},i})^2 - (h_z - \alpha k_y)^2 = 0, \tag{9a}$$
$$(-H_i^{\mathrm{h}} - E)^2 - h_x^2 - (h_y - \alpha k_{\mathrm{h},i})^2 - (h_z + \alpha k_y)^2 = 0. \tag{9b}$$

The scattering states in each different regions of the junction can be constructed from the linear combination of the corresponding propagating modes in each different regions. For example, for spin-up electronlike quasi-particles incident from the left superconductor lead, the wave functions of the scattering states in the left superconductor lead can be expressed as follows:

$$\Psi(z<0) = \psi_{\mathrm{r,e},\uparrow} + r_1 \psi_{\mathrm{l,h},\uparrow} + r_2 \psi_{\mathrm{l,e},\uparrow} + r_3 \psi_{\mathrm{l,h},\downarrow} + r_4 \psi_{\mathrm{l,e},\downarrow}, \tag{10}$$

where r_1 (r_3) are the Andreev reflection coefficients without (with) spin flip and r_2 (r_4) the normal reflection coefficients without (with) spin flip, respectively. In the bridge region between two superconductor leads, the wave functions of the scattering states can be expressed as

$$\Psi(0<z<L) = a_1^{\mathrm{e}} \psi_{\mathrm{e},1} + a_2^{\mathrm{e}} \psi_{\mathrm{e},2} + a_3^{\mathrm{e}} \psi_{\mathrm{e},3} + a_4^{\mathrm{e}} \psi_{\mathrm{e},4} + a_1^{\mathrm{h}} \psi_{\mathrm{h},1} + a_2^{\mathrm{h}} \psi_{\mathrm{h},2} + a_3^{\mathrm{h}} \psi_{\mathrm{h},3} + a_4^{\mathrm{h}} \psi_{\mathrm{h},4}, \tag{11}$$

where $a_{i=1\sim4}^{\mathrm{e\ (h)}}$ are the scattering coefficients corresponding to the four electron (hole) propagating modes in the bridge region, respectively. In the right superconductor lead, the wave functions of the scattering states can be expressed as

$$\Psi(z>L) = t_1 \psi_{\mathrm{l,h},\uparrow} + t_2 \psi_{\mathrm{l,e},\uparrow} + t_3 \psi_{\mathrm{l,h},\downarrow} + t_4 \psi_{\mathrm{l,e},\downarrow}, \tag{12}$$

where $t_{i=1\sim4}$ are the transmission coefficients. All the scattering coefficients in the wavefunctions (10)–(12) are determined by the interfacial boundary conditions at $z = 0$ and L, which are

$$\Psi(0^-) = \Psi(0^+), \tag{13}$$
$$\Psi(L+0^-) = \Psi(L+0^+), \tag{14}$$
$$\hat{v}_z \Psi(0^-) = \hat{v}_z \Psi(0^+), \tag{15}$$
$$\hat{v}_z \Psi(L+0^-) = \hat{v}_z \Psi(L+0^+), \tag{16}$$

where

$$\hat{v}_z = \frac{1}{\hbar} \frac{\partial \hat{H}_{\mathrm{BdG}}}{\partial k_z}$$

is the velocity operator.

By the procedure outlined above, for a fixed quasi-particle excitation energy E and k_y, the wavefunctions corresponding to various scattering processes can be constructed in a similar form. On the basis of these wavefunctions, we can construct the retarded Green's functions $G^{\mathrm{R}}(z,z';E,k_y)$ following McMillans' method.[39] To construct the retarded Green's functions, we need the wavefunctions and the conjugates of all relevant outgoing waves due to various types of scattering processes and the conjugate processes. Let us take the retarded Green's function in the left superconductor lead region (with $z,z' < 0$) as the example. In this region, for electronlike or holelike quasi-particles incident from the left or from the right superconductor lead, there are eight different types of outgoing waves in total, and the corresponding scattering wavefunctions can be expressed as follows:

$$\psi_1(z) = \hat{A}_1 \mathrm{e}^{\mathrm{i}k_\mathrm{e}z+\mathrm{i}k_y y} + a_1\hat{A}_4 \mathrm{e}^{\mathrm{i}k_\mathrm{h}z+\mathrm{i}k_y y} + b_1\hat{A}_3 \mathrm{e}^{-\mathrm{i}k_\mathrm{e}z+\mathrm{i}k_y y} + c_1\hat{B}_4 \mathrm{e}^{\mathrm{i}k_\mathrm{h}z+\mathrm{i}k_y y} + d_1\hat{B}_3 \mathrm{e}^{-\mathrm{i}k_\mathrm{e}z+\mathrm{i}k_y y}, \tag{17a}$$

$$\psi_2(z) = \hat{A}_2 \mathrm{e}^{-\mathrm{i}k_\mathrm{h}z+\mathrm{i}k_y y} + a_2\hat{A}_3 \mathrm{e}^{-\mathrm{i}k_\mathrm{e}z+\mathrm{i}k_y y} + b_2\hat{A}_4 \mathrm{e}^{\mathrm{i}k_\mathrm{h}z+\mathrm{i}k_y y} + c_2\hat{B}_3 \mathrm{e}^{-\mathrm{i}k_\mathrm{e}z+\mathrm{i}k_y y} + d_2\hat{B}_4 \mathrm{e}^{\mathrm{i}k_\mathrm{h}z+\mathrm{i}k_y y}, \tag{17b}$$

$$\psi_3(z) = \hat{B}_1 \mathrm{e}^{\mathrm{i}k_\mathrm{e}z+\mathrm{i}k_y y} + a_3\hat{B}_4 \mathrm{e}^{\mathrm{i}k_\mathrm{h}z+\mathrm{i}k_y y} + b_3\hat{B}_3 \mathrm{e}^{-\mathrm{i}k_\mathrm{e}z+\mathrm{i}k_y y} + c_3\hat{A}_4 \mathrm{e}^{\mathrm{i}k_\mathrm{h}z+\mathrm{i}k_y y} + d_3\hat{A}_3 \mathrm{e}^{-\mathrm{i}k_\mathrm{e}z+\mathrm{i}k_y y}, \tag{17c}$$

$$\psi_4(z) = \hat{B}_2 \mathrm{e}^{-\mathrm{i}k_\mathrm{h}z+\mathrm{i}k_y y} + a_4\hat{B}_3 \mathrm{e}^{-\mathrm{i}k_\mathrm{e}z+\mathrm{i}k_y y} + b_4\hat{B}_4 \mathrm{e}^{\mathrm{i}k_\mathrm{h}z+\mathrm{i}k_y y} + c_4\hat{A}_3 \mathrm{e}^{-\mathrm{i}k_\mathrm{e}z+\mathrm{i}k_y y} + d_4\hat{A}_4 \mathrm{e}^{\mathrm{i}k_\mathrm{h}z+\mathrm{i}k_y y}, \tag{17d}$$

$$\psi_5(z) = e_1\hat{A}_3 \mathrm{e}^{-\mathrm{i}k_\mathrm{e}z+\mathrm{i}k_y y} + f_1\hat{A}_4 \mathrm{e}^{\mathrm{i}k_\mathrm{h}z+\mathrm{i}k_y y} + g_1\hat{B}_3 \mathrm{e}^{-\mathrm{i}k_\mathrm{e}z+\mathrm{i}k_y y} + h_1\hat{B}_4 \mathrm{e}^{\mathrm{i}k_\mathrm{h}z+\mathrm{i}k_y y}, \tag{17e}$$

$$\psi_6(z) = e_2\hat{A}_4 \mathrm{e}^{\mathrm{i}k_\mathrm{h}z+\mathrm{i}k_y y} + f_2\hat{A}_3 \mathrm{e}^{-\mathrm{i}k_\mathrm{e}z+\mathrm{i}k_y y} + g_2\hat{B}_4 \mathrm{e}^{\mathrm{i}k_\mathrm{h}z+\mathrm{i}k_y y} + h_2\hat{B}_3 \mathrm{e}^{-\mathrm{i}k_\mathrm{e}z+\mathrm{i}k_y y}, \tag{17f}$$

$$\psi_7(z) = e_3\hat{B}_3 \mathrm{e}^{-\mathrm{i}k_\mathrm{e}z+\mathrm{i}k_y y} + f_3\hat{B}_4 \mathrm{e}^{\mathrm{i}k_\mathrm{h}z+\mathrm{i}k_y y} + g_3\hat{A}_3 \mathrm{e}^{-\mathrm{i}k_\mathrm{e}z+\mathrm{i}k_y y} + h_3\hat{A}_4 \mathrm{e}^{\mathrm{i}k_\mathrm{h}z+\mathrm{i}k_y y}, \tag{17g}$$

$$\psi_8(z) = e_4\hat{B}_4 \mathrm{e}^{\mathrm{i}k_\mathrm{h}z+\mathrm{i}k_y y} + f_4\hat{B}_3 \mathrm{e}^{-\mathrm{i}k_\mathrm{e}z+\mathrm{i}k_y y} + g_4\hat{A}_4 \mathrm{e}^{\mathrm{i}k_\mathrm{h}z+\mathrm{i}k_y y} + h_4\hat{A}_3 \mathrm{e}^{-\mathrm{i}k_\mathrm{e}z+\mathrm{i}k_y y}, \tag{17h}$$

where $\psi_{1\sim4}$ represent the scattering processes when spin-up electronlike quasi-particles, spin-up holelike quasi-particles, spin-down electronlike quasi-particles, and spin-down holelike quasi-particles are incident from the left superconductor leads, respectively, while $\psi_{5\sim8}$ represent the corresponding scattering processes when quasi-particles are incident from the right superconductor leads, respectively. The coefficients a_i (c_i) are the Andreev reflection amplitudes without (with) spin flip and b_i (d_i) the normal reflection amplitudes without (with) spin flip, respectively. The coefficients e_i, f_i, g_i, and h_i are the transmission amplitudes. All these coefficients are determined by the interfacial boundary conditions (13)–(16) for the corresponding wave functions. Similarly, in terms of the eigensolutions of the conjugated BdG Hamiltonian, the conjugated wavefunctions corresponding to the conjugate processes of the eight different types of scattering processes described above can be expressed as follows:

$$\bar{\psi}_1(z') = \hat{C}_1 \mathrm{e}^{\mathrm{i}k_\mathrm{e}z'-\mathrm{i}k_y y} + a_1'\hat{C}_4 \mathrm{e}^{\mathrm{i}k_\mathrm{h}z'-\mathrm{i}k_y y} + b_1'\hat{C}_3 \mathrm{e}^{-\mathrm{i}k_\mathrm{e}z'-\mathrm{i}k_y y} + c_1'\hat{D}_4 \mathrm{e}^{\mathrm{i}k_\mathrm{h}z'-\mathrm{i}k_y y} + d_1'\hat{D}_3 \mathrm{e}^{-\mathrm{i}k_\mathrm{e}z'-\mathrm{i}k_y y}, \tag{18a}$$

$$\bar{\psi}_2(z') = \hat{C}_2 \mathrm{e}^{-\mathrm{i}k_\mathrm{h}z'-\mathrm{i}k_y y} + a_2'\hat{C}_3 \mathrm{e}^{-\mathrm{i}k_\mathrm{e}z'-\mathrm{i}k_y y} + b_2'\hat{C}_4 \mathrm{e}^{\mathrm{i}k_\mathrm{h}z'-\mathrm{i}k_y y} + c_2'\hat{D}_3 \mathrm{e}^{-\mathrm{i}k_\mathrm{e}z'-\mathrm{i}k_y y} + d_2'\hat{D}_4 \mathrm{e}^{\mathrm{i}k_\mathrm{h}z'-\mathrm{i}k_y y}, \tag{18b}$$

$$\bar{\psi}_3(z') = \hat{D}_1 \mathrm{e}^{\mathrm{i}k_\mathrm{e}z'+\mathrm{i}k_y y} + a_3'\hat{D}_4 \mathrm{e}^{\mathrm{i}k_\mathrm{h}z'-\mathrm{i}k_y y} + b_3'\hat{D}_3 \mathrm{e}^{-\mathrm{i}k_\mathrm{e}z'-\mathrm{i}k_y y} + c_3'\hat{C}_4 \mathrm{e}^{\mathrm{i}k_\mathrm{h}z'-\mathrm{i}k_y y} + d_3'\hat{C}_3 \mathrm{e}^{-\mathrm{i}k_\mathrm{e}z'-\mathrm{i}k_y y}, \tag{18c}$$

$$\bar{\psi}_4(z') = \hat{D}_2 \mathrm{e}^{-\mathrm{i}k_\mathrm{h}z'+\mathrm{i}k_y y} + a_4'\hat{D}_3 \mathrm{e}^{-\mathrm{i}k_\mathrm{e}z'-\mathrm{i}k_y y} + b_4'\hat{D}_4 \mathrm{e}^{\mathrm{i}k_\mathrm{h}z'-\mathrm{i}k_y y} + c_4'\hat{C}_3 \mathrm{e}^{-\mathrm{i}k_\mathrm{e}z'-\mathrm{i}k_y y} + d_4'\hat{C}_4 \mathrm{e}^{\mathrm{i}k_\mathrm{h}z'-\mathrm{i}k_y y}, \tag{18d}$$

$$\bar{\psi}_5(z') = e_1'\hat{C}_3 \mathrm{e}^{-\mathrm{i}k_\mathrm{e}z'-\mathrm{i}k_y y} + f_1'\hat{C}_4 \mathrm{e}^{\mathrm{i}k_\mathrm{h}z'-\mathrm{i}k_y y} + g_1'\hat{D}_3 \mathrm{e}^{-\mathrm{i}k_\mathrm{e}z'-\mathrm{i}k_y y} + h_1'\hat{D}_4 \mathrm{e}^{\mathrm{i}k_\mathrm{h}z'-\mathrm{i}k_y y}, \tag{18e}$$

$$\bar{\psi}_6(z') = e_2'\hat{C}_4 \mathrm{e}^{\mathrm{i}k_\mathrm{h}z'-\mathrm{i}k_y y} + f_2'\hat{C}_3 \mathrm{e}^{-\mathrm{i}k_\mathrm{e}z'-\mathrm{i}k_y y} + g_2'\hat{D}_4 \mathrm{e}^{\mathrm{i}k_\mathrm{h}z'-\mathrm{i}k_y y} + h_2'\hat{D}_3 \mathrm{e}^{-\mathrm{i}k_\mathrm{e}z'-\mathrm{i}k_y y}, \tag{18f}$$

$$\bar{\psi}_7(z') = e_3'\hat{D}_3 \mathrm{e}^{-\mathrm{i}k_\mathrm{e}z'-\mathrm{i}k_y y} + f_3'\hat{D}_4 \mathrm{e}^{\mathrm{i}k_\mathrm{h}z'-\mathrm{i}k_y y} + g_3'\hat{C}_3 \mathrm{e}^{-\mathrm{i}k_\mathrm{e}z'-\mathrm{i}k_y y} + h_3'\hat{C}_4 \mathrm{e}^{\mathrm{i}k_\mathrm{h}z'-\mathrm{i}k_y y}, \tag{18g}$$

$$\bar{\psi}_8(z') = e_4'\hat{D}_4 \mathrm{e}^{\mathrm{i}k_\mathrm{h}z'-\mathrm{i}k_y y} + f_4'\hat{D}_3 \mathrm{e}^{-\mathrm{i}k_\mathrm{e}z'-\mathrm{i}k_y y} + g_4'\hat{C}_4 \mathrm{e}^{\mathrm{i}k_\mathrm{h}z'-\mathrm{i}k_y y} + h_4'\hat{C}_3 \mathrm{e}^{-\mathrm{i}k_\mathrm{e}z'-\mathrm{i}k_y y}, \tag{18h}$$

where $\hat{C}_{i=1\sim4}$ and $\hat{D}_{i=1\sim4}$ are the spinors determined by the conjugated BdG Hamiltonian, with

$$\hat{C}_1 = \begin{bmatrix} u_2e_2 \\ 0 \\ 0 \\ v_2 \end{bmatrix}, \quad \hat{C}_2 = \begin{bmatrix} v_1e_1 \\ 0 \\ 0 \\ u_1 \end{bmatrix}, \quad \hat{C}_3 = \begin{bmatrix} u_1e_1 \\ 0 \\ 0 \\ v_1 \end{bmatrix}, \quad \hat{C}_4 = \begin{bmatrix} v_2e_2 \\ 0 \\ 0 \\ u_2 \end{bmatrix}, \tag{19a}$$

$$\hat{D}_1 = \begin{bmatrix} 0 \\ -u_2e_2 \\ v_2 \\ 0 \end{bmatrix}, \quad \hat{D}_2 = \begin{bmatrix} 0 \\ -v_1e_1 \\ u_1 \\ 0 \end{bmatrix}, \quad \hat{D}_3 = \begin{bmatrix} 0 \\ -u_1e_1 \\ v_1 \\ 0 \end{bmatrix}, \quad \hat{D}_4 = \begin{bmatrix} 0 \\ -v_2e_2 \\ u_2 \\ 0 \end{bmatrix}. \tag{19b}$$

All the coefficients in Eqs. (18a)–(18h) are also determined by the interfacial boundary conditions (13)–(16) for the corresponding wave functions. After all the relevant wavefunctions in Eqs. (17)–(18) are determined by the interfacial boundary conditions at $z = 0$ and $z = L$, the retarded Green's functions $G^\mathrm{R}(z,z';E,k_y)$ in the left superconductor lead region (with $z,z' < 0$) can be constructed from a linear combination of $\psi_i(z)\bar{\psi}_j(z')^\mathrm{T}$, which are 4×4 matrices in Nambu-spin space and can be expressed explicitly as follows:

$$G^\mathrm{R}(z,z';E,k_y) = \sum_{ij} g_{ij}\psi_i(z)\bar{\psi}_j(z')^\mathrm{T} = \begin{bmatrix} G_\mathrm{ee}(z,z';E,k_y) & G_\mathrm{eh}(z,z';E,k_y) \\ G_\mathrm{he}(z,z';E,k_y) & G_\mathrm{hh}(z,z';E,k_y) \end{bmatrix}, \tag{20}$$

where $i = 1\sim4$ and $j = 5\sim8$ if $z > z'$, $i = 5\sim8$ and $j = 1\sim4$ if $z < z'$, and $G_{\alpha\beta}$ ($\alpha,\beta \in \{\mathrm{e},\mathrm{h}\}$) are 2×2 matrices in spin space and their elements are denoted as $G_{\alpha\beta,\nu\delta}$, with $\nu,\delta = \uparrow,\downarrow$. For simplicity, in the following we denote $G^\mathrm{R}(z,z';E,k_y)$ simply as $G(z,z')$. The Green's functions so constructed satisfy the following equation of motion: $[E - \hat{H}_\mathrm{BdG}(z)]G(z,z') =$

$\delta(z-z')$. By integrating this equation at $z=z'$, the following boundary conditions can be obtained for $G(z,z')$ at $z=z'$,

$$G(z,z-0)=G(z,z+0), \tag{21}$$

$$\frac{\partial}{\partial z}G(z,z-0)-\frac{\partial}{\partial z}G(z,z+0)=\frac{2m}{\hbar^2}\sigma_0\tau_z, \tag{22}$$

where τ_z represent the Pauli matrices in Nambu space. The coefficients g_{ij} in Eq. (20) are determined by the boundary conditions (21)–(22).

There are 16 elements in total in the retarded Green's function matrix $G(z,z')$. From the expressions of the current operator in the superconductor lead regions (see Eqs. (28)–(29) below), one can see that the elements $G_{\mathrm{ee},\uparrow\downarrow}$, $G_{\mathrm{ee},\downarrow\uparrow}$, $G_{\mathrm{hh},\uparrow\downarrow}$, $G_{\mathrm{hh},\downarrow\uparrow}$, $G_{\mathrm{eh},\uparrow\uparrow}$, $G_{\mathrm{eh},\downarrow\downarrow}$, $G_{\mathrm{he},\uparrow\uparrow}$, and $G_{\mathrm{he},\downarrow\downarrow}$ are not involved in the calculations when we calculate the charge current in the superconductor lead regions using the retarded Green's function matrix. Due to this fact, the expressions of $G(z,z')$ can be simplified substantially by setting these uninvolved elements to zero. By this simplification, we find that $G(z,z')$ defined by Eq. (20) can be equivalently expressed as the sum of two different parts: $G(z,z')=G^{(\uparrow)}(z,z')+G^{(\downarrow)}(z,z')$, where $G^{(\uparrow)}(z,z')$ and $G^{(\downarrow)}(z,z')$ are 4×4 matrices in Nambu-spin space and can be expressed by a set of simplified outgoing wavefunctions and the conjugates which take into account the contributions of spin-up and spin-down propagating modes separately. For instance, in the left superconductor lead region $G^{(\uparrow)}(z,z')$ can be expressed by the following simplified forms of the wavefunctions ψ_1, ψ_2, ψ_5, and ψ_6, which are given in Eqs. (17a)–(17h) and their conjugates are given in Eqs. (18a)–(18h),

$$\psi_1(z)=\hat{A}_1\,\mathrm{e}^{\mathrm{i}k_\mathrm{e}z+\mathrm{i}k_y y}+a_1\hat{A}_4\,\mathrm{e}^{\mathrm{i}k_\mathrm{h}z+\mathrm{i}k_y y}+b_1\hat{A}_3\,\mathrm{e}^{-\mathrm{i}k_\mathrm{e}z+\mathrm{i}k_y y}, \tag{23a}$$

$$\psi_2(z)=\hat{A}_2\,\mathrm{e}^{-\mathrm{i}k_\mathrm{h}z+\mathrm{i}k_y y}+a_2\hat{A}_3\,\mathrm{e}^{-\mathrm{i}k_\mathrm{e}z+\mathrm{i}k_y y}+b_2\hat{A}_4\,\mathrm{e}^{\mathrm{i}k_\mathrm{h}z+\mathrm{i}k_y y}, \tag{23b}$$

$$\psi_5(z)=e_1\hat{A}_3\,\mathrm{e}^{-\mathrm{i}k_\mathrm{e}z+\mathrm{i}k_y y}+f_1\hat{A}_4\,\mathrm{e}^{\mathrm{i}k_\mathrm{h}z+\mathrm{i}k_y y}, \tag{23c}$$

$$\psi_6(z)=e_2\hat{A}_4\,\mathrm{e}^{\mathrm{i}k_\mathrm{h}z+\mathrm{i}k_y y}+f_2\hat{A}_3\,\mathrm{e}^{-\mathrm{i}k_\mathrm{e}z+\mathrm{i}k_y y}, \tag{23d}$$

$$\bar{\psi}_1(z')=\hat{C}_1\,\mathrm{e}^{\mathrm{i}k_\mathrm{e}z'-\mathrm{i}k_y y}+a_1'\hat{C}_4\,\mathrm{e}^{\mathrm{i}k_\mathrm{h}z'-\mathrm{i}k_y y}+b_1'\hat{C}_3\,\mathrm{e}^{-\mathrm{i}k_\mathrm{e}z'-\mathrm{i}k_y y}, \tag{23e}$$

$$\bar{\psi}_2(z')=\hat{C}_2\,\mathrm{e}^{-\mathrm{i}k_\mathrm{h}z'-\mathrm{i}k_y y}+a_2'\hat{C}_3\,\mathrm{e}^{-\mathrm{i}k_\mathrm{e}z'-\mathrm{i}k_y y}+b_2'\hat{C}_4\,\mathrm{e}^{\mathrm{i}k_\mathrm{h}z'-\mathrm{i}k_y y}, \tag{23f}$$

$$\bar{\psi}_5(z')=e_1'\hat{C}_3\,\mathrm{e}^{-\mathrm{i}k_\mathrm{e}z'-\mathrm{i}k_y y}+f_1'\hat{C}_4\,\mathrm{e}^{\mathrm{i}k_\mathrm{h}z'-\mathrm{i}k_y y}, \tag{23g}$$

$$\bar{\psi}_6(z')=e_2'\hat{C}_4\,\mathrm{e}^{\mathrm{i}k_\mathrm{h}z'-\mathrm{i}k_y y}+f_2'\hat{C}_3\,\mathrm{e}^{-\mathrm{i}k_\mathrm{e}z'-\mathrm{i}k_y y}. \tag{23h}$$

But it should be stressed that all scattering coefficients in these simplified wavefunctions and the conjugates, including a_i, b_i, e_i, f_i, a_i', b_i', e_i', and f_i', should still be calculated by use of the complete scattering wavefunctions given in Eqs. (17a)–(17h) and the conjugates given in Eqs. (18a)–(18h), which in combination with the interfacial boundary conditions (13)–(16) include not only the effect of all spin-conserving interfacial scattering processes but also the effect of all spin-flip interfacial scattering processes. The equation set Eqs. (23a)–(23h) only means that some elements of $G(z,z')$ can be obtained equivalently by use of the above simplified forms of ψ_1, ψ_2, ψ_5, and ψ_6 and the conjugates. Due to the presence of spin-orbit coupling and Zeeman splitting in the bridge region, the spin-up and spin-down scattering processes should be treated as a whole but cannot be treated separately as simplified in the equation set Eqs. (23a)–(23h).

Substituting Eqs. (23a)–(23h) into Eq. (20), we find that in the left superconductor lead region $G^{(\uparrow)}(z,z')$ can be expressed in the following explicit forms:

$$G^{(\uparrow)}(z,z')=\alpha_1\psi_1(z)\bar{\psi}_5^{\mathrm{T}}(z')+\alpha_2\psi_1(z)\bar{\psi}_6^{\mathrm{T}}(z')+\alpha_3\psi_2(z)\bar{\psi}_5^{\mathrm{T}}(z')+\alpha_4\psi_2(z)\bar{\psi}_6^{\mathrm{T}}(z') \tag{24a}$$

for $z'<z<0$, and

$$G^{(\uparrow)}(z,z')=\beta_1\psi_5(z)\bar{\psi}_1^{\mathrm{T}}(z')+\beta_2\psi_6(z)\bar{\psi}_1^{\mathrm{T}}(z')+\beta_3\psi_5(z)\bar{\psi}_2^{\mathrm{T}}(z')+\beta_4\psi_6(z)\bar{\psi}_2^{\mathrm{T}}(z') \tag{24b}$$

for $z<z'<0$. In Eqs. (24a) and (24b), the coefficients $\alpha_{i=1\sim4}$ and $\beta_{i=1\sim4}$ are determined by the boundary conditions (21)–(22) for the Green's functions at $z=z'$. Making use of these boundary conditions and after some straightforward algebras, $G^{(\uparrow)}(z,z')$ can be further simplified to the following form (for $z'<z<0$):

$$\begin{aligned}G^{(\uparrow)}(z,z')=\;&j_1[\hat{A}_1\hat{C}_3^{\mathrm{T}}\,\mathrm{e}^{\mathrm{i}k_\mathrm{e}(z-z')}+a_1\hat{A}_4\hat{C}_3^{\mathrm{T}}\,\mathrm{e}^{\mathrm{i}k_\mathrm{h}z-\mathrm{i}k_\mathrm{e}z'}+b_1\hat{A}_3\hat{C}_3^{\mathrm{T}}\,\mathrm{e}^{-\mathrm{i}k_\mathrm{e}z-\mathrm{i}k_\mathrm{e}z'}]\\&+j_2[\hat{A}_2\hat{C}_4^{\mathrm{T}}\,\mathrm{e}^{-\mathrm{i}k_\mathrm{h}(z-z')}+a_2\hat{A}_3\hat{C}_4^{\mathrm{T}}\,\mathrm{e}^{-\mathrm{i}k_\mathrm{e}z+\mathrm{i}k_\mathrm{h}z'}+b_2\hat{A}_4\hat{C}_4^{\mathrm{T}}\,\mathrm{e}^{\mathrm{i}k_\mathrm{h}z+\mathrm{i}k_\mathrm{h}z'}],\end{aligned} \tag{25}$$

where $\hat{A}_{i=1\sim4}$ are the spinors defined in Eq. (4) and $\hat{C}_{i=1\sim4}^{\mathrm{T}}$ the transposes of the spinors defined in Eq. (19a), and j_1 and j_2 are two coefficients defined by

$$j_1=\frac{mE}{\mathrm{i}\hbar^2k_\mathrm{e}\Omega_1},\quad j_2=\frac{mE}{\mathrm{i}\hbar^2k_\mathrm{h}\Omega_2}. \tag{26}$$

Similarly, by the same procedure as above, we find that in the left superconductor lead region $G^{(\downarrow)}(z,z')$ can be expressed in the following explicit forms (for $z'<z<0$),

$$G^{(\downarrow)}(z,z') = j_1[\hat{B}_1\hat{D}_3^{\mathrm{T}}\mathrm{e}^{\mathrm{i}k_{\mathrm{e}}(z-z')} + a_1\hat{B}_4\hat{D}_3^{\mathrm{T}}\mathrm{e}^{\mathrm{i}k_{\mathrm{h}}z-\mathrm{i}k_{\mathrm{e}}z'} + b_1\hat{B}_3\hat{D}_3^{\mathrm{T}}\mathrm{e}^{-\mathrm{i}k_{\mathrm{e}}z-\mathrm{i}k_{\mathrm{e}}z'}] + j_2[\hat{B}_2\hat{D}_4^{\mathrm{T}}\mathrm{e}^{-\mathrm{i}k_{\mathrm{h}}(z-z')} + a_2\hat{B}_3\hat{D}_4^{\mathrm{T}}\mathrm{e}^{-\mathrm{i}k_{\mathrm{e}}z+\mathrm{i}k_{\mathrm{h}}z'} + b_2\hat{B}_4\hat{D}_4^{\mathrm{T}}\mathrm{e}^{\mathrm{i}k_{\mathrm{h}}z+\mathrm{i}k_{\mathrm{h}}z'}], \tag{27}$$

where $\hat{B}_{i=1\sim4}$ are the spinors defined in Eq. (7) and $\hat{D}^{\mathrm{T}}_{i=1\sim4}$ are the transposes of the spinors defined in Eq. (19b). The advanced Green's functions can be constructed by incoming waves in a similar way as above.

After all the relevant Green's function matrices are obtained, the Josephson current in the superconductor leads can be calculated from them.[40,41] Firstly, we derive the charge current density operator from the charge density operator, which reads

$$\hat{\rho} = -\frac{1}{2}e\hat{\Psi}^{\dagger}(z)\sigma_0\tau_z\hat{\Psi}(z'),$$

where $\hat{\Psi}^{\dagger}(z)$ and $\hat{\Psi}(z')$ are the field operators and e the electron charge and $z=z'+0$. From the time derivative of the charge density operator, the following continuity equation are obtained:

$$\frac{\partial}{\partial t}\hat{\rho} + \nabla\hat{J} + \hat{S} = 0,$$

where $\hat{J}$ is the quasi-particle part of the charge current density operator and $\hat{S}$ is the source term (The physical origin of the source term is due to the non-self-consistency of the mean-field treatment of Cooper pairing states. In a fully self-consistent calculation, the source term is vanished. See, *e.g.*, Refs. [43–46]), which are given respectively by

$$\hat{J} = \frac{e\hbar}{4\mathrm{i}m}(\frac{\partial}{\partial z} - \frac{\partial}{\partial z'})[\hat{\psi}^{+}_{\uparrow}(z)\hat{\psi}_{\uparrow}(z') + \hat{\psi}^{+}_{\downarrow}(z)\hat{\psi}_{\downarrow}(z') + \hat{\psi}_{\uparrow}(z)\hat{\psi}^{+}_{\uparrow}(z') + \hat{\psi}_{\downarrow}(z)\hat{\psi}^{+}_{\downarrow}(z')], \tag{28}$$

$$\hat{S} = -\frac{e}{2\mathrm{i}\hbar}(\hat{\Delta}(z) + \hat{\Delta}(z'))[\hat{\psi}_{\downarrow}(z)\hat{\psi}_{\uparrow}(z') - \hat{\psi}^{+}_{\uparrow}(z)\hat{\psi}^{+}_{\downarrow}(z') - \hat{\psi}_{\uparrow}(z)\hat{\psi}_{\downarrow}(z') + \hat{\psi}^{+}_{\downarrow}(z)\hat{\psi}^{+}_{\uparrow}(z')], \tag{29}$$

where the superconducting paring potential operators $\hat{\Delta}(z)$ and $\hat{\Delta}(z')$ act on the field operators $\hat{\Psi}^{\dagger}(z)$ and $\hat{\Psi}(z')$, respectively. The Josephson current is given by $I = \langle\hat{J}\rangle + \int\langle\hat{S}\rangle\mathrm{d}z$, where $\langle\hat{J}\rangle$ and $\langle\hat{S}\rangle$ denote the expectation values of $\hat{J}$ and $\hat{S}$, which can be obtained by summing all the relevant contributions from the relevant Green's function matrix elements. After some straightforward but cumbersome algebras, the total Josephson current can be expressed in the following explicit form:

$$I = \frac{ek_{\mathrm{B}}T}{2\hbar}\int \mathrm{d}k_y\Sigma_{\omega_n}\left[\frac{k_{\mathrm{e}}+k_{\mathrm{h}}}{k_{\mathrm{e}}}\frac{|\,\Delta(\theta)\,|}{\sqrt{\omega_n^2+|\,\Delta(\theta)\,|^2}}(a_1+a_3) - \frac{k_{\mathrm{e}}+k_{\mathrm{h}}}{k_{\mathrm{h}}}\frac{|\,\Delta(\pi-\theta)\,|}{\sqrt{\omega_n^2+|\,\Delta(\pi-\theta)\,|^2}}(a_2+a_4)\right], \tag{30}$$

where the energy argument is analytically continued to the Matsbura frequencies $\omega_n = \mathrm{i}(2n+1)\pi/\beta$. On the basis of this formula, we can calculate the the Josephson current and the current-phase relation under various different situations by means of numerical methods.

3. Results and discussion

In the following we present the numerical results obtained based on the formalism outlined above. For convenience, in the results presented below, the magnitudes of all relevant quantities are given in dimensionless forms as following: the strength of Rashba SOC is measured by a dimensionless quantity $\alpha \equiv 2m\alpha_{\mathrm{R}}/\hbar^2k_{\mathrm{F}}$, the strength of Zeeman splitting and superconducting paring potential are measured in units of the chemical potential μ, the magnitude of the Josephson current is measured in units of $e\Delta_0/\hbar$, the width L of the bridge region between two superconductor leads is measured in units of the superconducting correlation length $\xi = \hbar^2k_{\mathrm{F}}/m\Delta_0$, and the temperature T is measured in units of the critical temperature T_{c}. We set $L = 0.1\xi$ and $T = 0.1T_{\mathrm{c}}$ in the numerical calculations.

A fundamental property of a Josephson junction is its current–phase relation (CPR). In general, the Josephson current can be decomposed into a Fourier series of contributions of different orders as following: $I(\phi) = \sum_{n\geq1}[I_n\sin(n\phi) + J_n\cos(n\phi)]$, where the current components with index n correspond to the contributions of the n-th reflection processes of quasi-particles.[42] If time reversal symmetry or inversion symmetry is conserved in the system, the coefficients J_n vanish for all n since in such cases $I(\phi) = -I(-\phi)$, and consequently no Josephson current can occur at zero phase bias. Furthermore, if the higher-order current components with index $n \geq 2$ are negligible, the CPR then reduces to the ordinary sinusoidal form, $I(\phi) \simeq I_{\mathrm{c}}\sin(\phi)$, with I_{c} the critical current. This is usually the case in the absence of spin–orbit coupling and Zeeman splitting. However, the presence of

spin–orbit coupling and Zeeman splitting would invalidate this simple argument. For the system under consideration, both time reversal symmetry and inversion symmetry can be simultaneously broken by tuning some relevant parameters of the system, including the relative orientations and the strengths of the Zeeman field and the spin–orbit field in the bridge region, the relative orientations between the a axes in two superconductor leads, or the relative orientations between the Zeeman field in the bridge region and the a axes in the superconductor leads. In the following discussions we focus on how the CPR varies as these relevant parameters are tuned. We show that the CPR of the system may exhibit a series of novel features due to the interplay of these complicated factors and anomalous Josephson current may occur at zero phase bias under various different situations when both time reversal symmetry and inversion symmetry of the system are simultaneously broken.

Since the pairing potentials in d-wave superconductors are anisotropic, the CPR of the considered structure would depend on the relative orientations of the a axes in two superconductor leads, which are characterized by the angles $a_{\rm L}$ and $a_{\rm R}$, respectively. We first consider the situations where the orientations of the $\boldsymbol{a}$ axes in two superconductor leads are parallel to each other and also parallel to the direction of the current flow, corresponding to that the angles $a_{\rm L} = a_{\rm R} = 0$. In Figs. 1(a)–1(c), we show several numerical results for the CPR obtained in such situations for various directions and strengths of the Zeeman field. For convenience of comparison, the values of all other parameters are set to be the same in all panels. Figure 1(a) shows that when the direction of the Zeeman field is along the x axis, the magnitude of the Josephson current can be changed significantly as the strength of the Zeeman field is varied, but the basic features of the CPR curves remain the sinusoidal-like forms and posses 2π periodicity in the phase bias ϕ, and though both time-reversal symmetry and inversion symmetry are broken in the cases shown there, no anomalous Josephson current occurs at zero phase bias. Just as usual, the first harmonic component $I_1\sin(\phi)$ plays the predominant role in the Josephson current in these cases and the contributions of other harmonics are negligible.

Figures 1(b) and 1(c) show that when the direction of the Zeeman field is along the y axis or along the z axis, both the magnitude of the Josephson current and some basic features of the CPR (*e.g.*, the periodicity in ϕ or the curve shapes of the CPR) may be significantly changed as the strength of the Zeeman field is varied, and furthermore, a finite anomalous Josephson current may occur at zero phase bias under some circumstances. For instance, in the cases of $h_y/\mu = 0.75$ and 1.0 in Fig. 1(b), the CPR possess a 2π-periodic dependence on the phase bias ϕ and no anomalous Josephson current occurs at $\phi = 0$. In these two cases, the first harmonic component $I_1\sin(\phi)$ plays the predominant role in the Josephson current and the first harmonic component $J_1\cos(\phi)$ is negligible as usual. In contrast, in the case of $h_y/\mu = 0.25$ in Fig. 1(b), though the CPR still possess 2π periodicity in ϕ, a finite anomalous Josephson current occurs at zero phase bias. In this case, the first harmonic component $I_1\sin(\phi)$ still plays the predominant role in the Josephson current, but the contribution of the first harmonic component $J_1\cos(\phi)$ is not negligible, while the higher-order current components with index $n \geq 2$ are still negligible. In the case of $h_y/\mu = 0.5$ in Fig. 1(b), the periodicity of the CPR in ϕ is no longer 2π but becomes to be π, and no anomalous Josephson current occurs at zero phase bias. From these features and the curve shape of the CPR in this case, one can see that the second harmonic component $I_2\sin(2\phi)$ plays the predominant role in the Josephson current in this case and the contributions of the two first harmonic components are negligible. Similar significant changes can also be found in the cases shown in Fig. 1(c). It is also noted that when the first harmonic components play the predominant role in the Josephson current, 0–π transitions may also be induced as the strength or the orientation of the Zeeman field is varied. For example, in the cases shown in Fig. 1(c), the CPR is typical of a π-state when $h_z/\mu = 0.75$ and typical of a 0-state when $h_z/\mu = 1.0$.

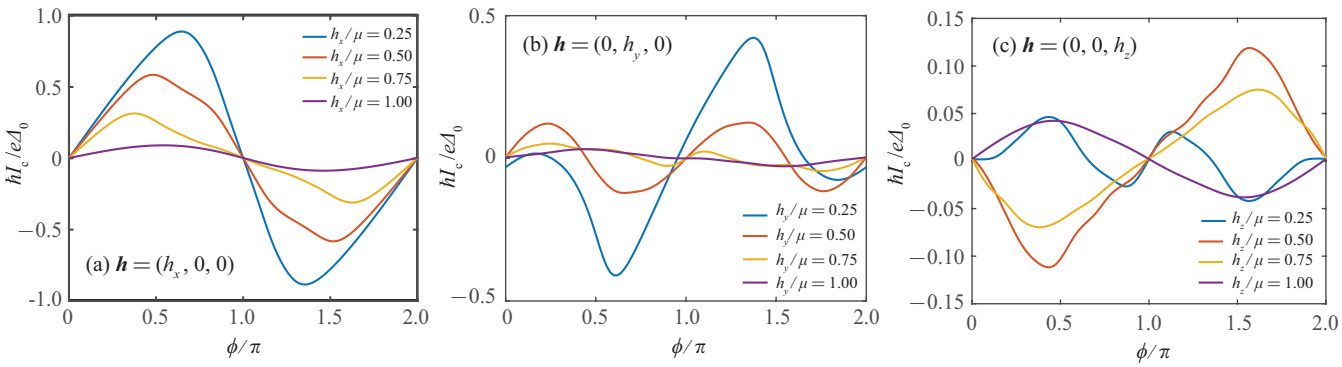


Fig. 1. The Josephson current as a function of the phase difference ϕ for various directions and strengths of the Zeeman field $\boldsymbol{h}$. In panels (a)–(c), the directions of the Zeeman field are set along the x axis, the y axis, and the z axis, respectively. The strengths of the Zeeman field are shown in the figures and the other parameters are set as $T = 0.1T_{\rm c}$, $L = 0.1\xi$, $\Delta_0 = 10^{-3}\mu$, $\alpha = 0.5$, $a_{\rm L} = 0$, $a_{\rm R} = 0$.

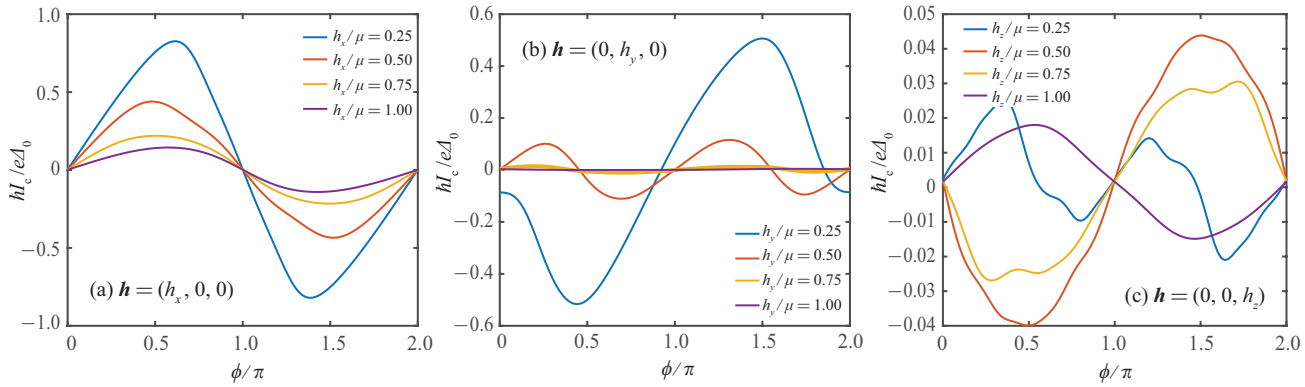


Fig. 2. The Josephson current as a function of the phase difference ϕ for various directions and strengths of the Zeeman field $\boldsymbol{h}$. In panels (a)–(c), the directions of the Zeeman field are set along the x axis, the y axis, and the z axis, respectively. The strengths of the Zeeman field are shown in the figures and the other parameters are set as $T=0.1T_c$, $L=0.1\xi$, $\Delta_0=10^{-3}\mu$, $\alpha=0.5$, $a_L=\pi/4$, $a_R=\pi/4$.

Next we consider the situations where the orientations of the $\boldsymbol{a}$ axes in two d-wave superconductor leads are still parallel to each other but misalign with the direction of the current flow. We take the situations where the angles $a_L=a_R=\pi/4$ as the examples. In Figs. 2(a)–2(c), we show several numerical results for the CPR obtained in such situations for various directions and strengths of the Zeeman field. For convenience of comparison, the values of all other parameters are set to be the same as in Figs. 1(a)–1(c). We can see that the basic features of the CPR shown in Figs. 2(a)–2(c) are largely similar as compared with the corresponding results shown in Figs. 1(a)–1(c). This suggests that if the orientations of the $\boldsymbol{a}$ axes in two superconductor leads keep parallel to each other, the changes of the relative orientations of the $\boldsymbol{a}$ axes in two superconductor leads with respect to the direction of the current flow has only some small influences on the basic features of the CPR, provided that the values of all other relevant parameters remain unchanged.

Now we consider the more complicated situations where the orientations of the a axes in two d-wave superconductor leads are not parallel to each other. We take the situations where the angles $a_L=0$ and $a_R=\pi/4$ as the examples. In such situations, the direction of the current flow is parallel to the a axis in the left superconductor lead but forms an angle of $\pi/4$ with the a axis in the right superconductor lead. In Figs. 3(a)–3(c) we show several numerical results for the CPR obtained in such situations for various directions and strengths of the Zeeman field. For convenience of comparison, the values of all other parameters are still set to be the same as in Figs. 1(a)–1(c) and 2(a)–2(c).

By comparing the corresponding results shown in Figs. 1–3, one can see that the CPR exhibits more rich and more complicated features in the situations illustrated in Fig. 3, and more significant changes may be induced both in the magnitude of the Josephson current and in some basic features of the CPR as the strength of the Zeeman field is varied. For instance, in the cases shown in Fig. 3(a), the periodicity of the CPR in ϕ is 2π and the Josephson current vanishes at $\phi=\pi/2$ and $\phi=3\pi/2$, but a finite anomalous Josephson current occurs at $\phi=0$. From these features and the shapes of the CPR curves in these cases, we can deduce that the Josephson current in these cases can be expressed approximately as a combination of the first harmonic component $J_1\cos(\phi)$ and the second harmonic component $I_2\sin(2\phi)$. Which component plays the predominant role in the Josephson current depends on the strength of the Zeeman splitting. For example, in the case of $h_x/\mu=0.25$, the second harmonic component $I_2\sin(2\phi)$ plays the predominant role, while in the case of $h_x/\mu=1$, the first harmonic component $J_1\cos(\phi)$ plays the predominant role.

In the cases shown in Fig. 3(b), when $h_y/\mu=0.25$, the periodicity of the CPR in ϕ is π and a small anomalous Josephson current occurs at zero phase bias. The Josephson current is also nonvanishing at $\phi=\pi/2$. From these features and the shape of the CPR curve in this case, we can deduce that the Josephson current in this case can be expressed approximately as a combination of the two second harmonic components $I_2\sin(2\phi)$ and $J_2\cos(2\phi)$, with the $I_2\sin(2\phi)$ component playing the predominant role. In contrast to the case of $h_y/\mu=0.25$, when $h_y/\mu=0.5$, 0.75, and 1.0, the periodicity of the CPR in ϕ is still π, but the Josephson current vanishes both at $\phi=\pi/2$ and at $\phi=0$ (*i.e.*, no anomalous Josephson current occurs at zero phase bias). From these features and the shapes of the CPR curves in these cases, we can deduce that the Josephson currents in these cases are predominated by the $I_2\sin(2\phi)$ component and the contributions of other harmonics are negligible.

In the cases shown in Fig. 3(c), the periodicity of the CPR in ϕ is 2π and a finite anomalous Josephson current occurs at zero phase bias in all the cases shown there. From the features of the CPR curves in these cases, we can deduce that the Josephson current in these cases can be expressed approximately as a combination of the first harmonic component $J_1\cos(\phi)$ and the second harmonic component $I_2\sin(2\phi)$. It

is also interesting to note that, since the magnitude of the anomalous Josephson current is determined by the first harmonic component $J_1\cos(\phi)$ in these cases, the magnitude of the anomalous Josephson current at zero phase bias in these cases is comparable to the maximum value of the Josephson current at $\phi \neq 0$.

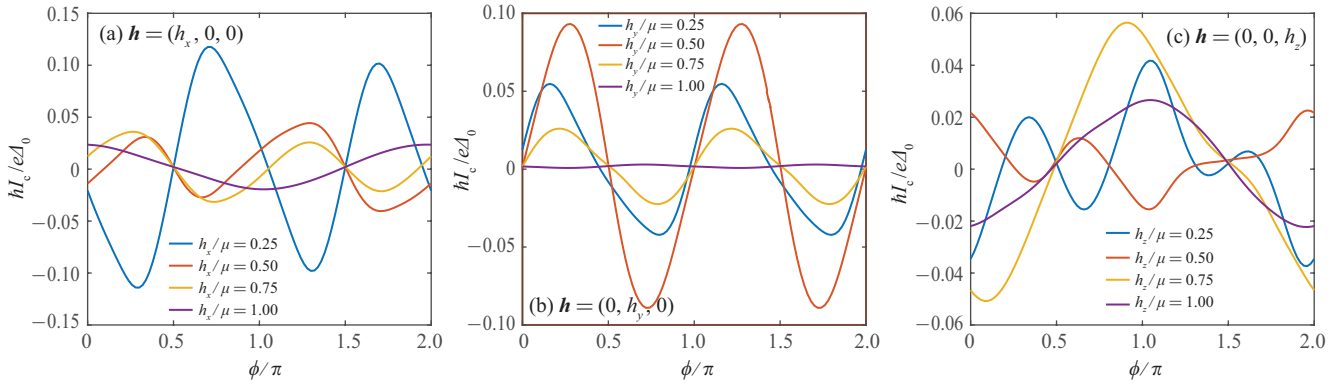


Fig. 3. The Josephson current as a function of the phase difference ϕ for various directions and strengths of the Zeeman field $\boldsymbol{h}$. In panels (a)–(c), the directions of the Zeeman field are set along the x axis, the y axis, and the z axis, respectively. The strengths of the Zeeman field are shown in the figures and the other parameters are set as $T = 0.1T_c$, $L = 0.1\xi$, $\Delta_0 = 10^{-3}\mu$, $\alpha = 0.5$, $a_L = 0$, $a_R = \pi/4$.

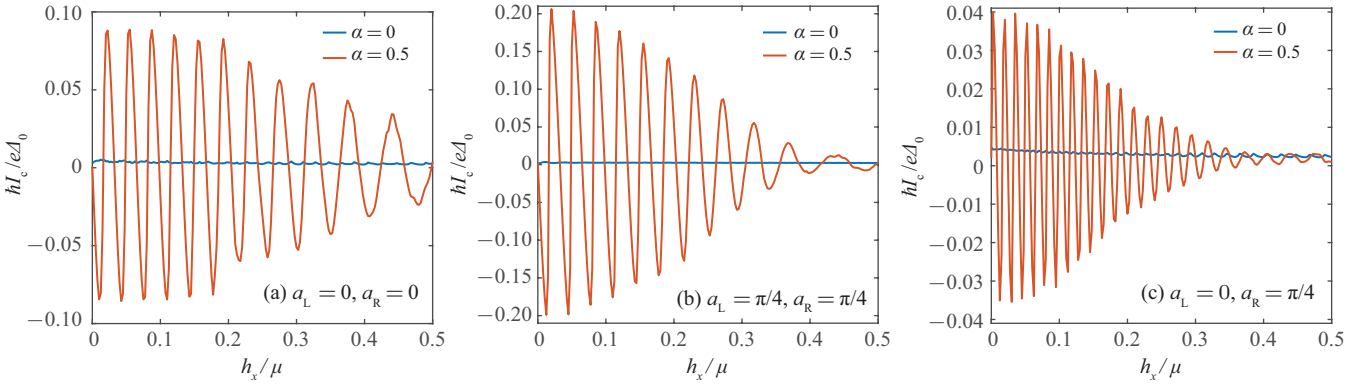


Fig. 4. The anomalous Josephson current I_a at zero phase bias as a function of the Zeeman field strength h_y for the Rashba SOC strength $\alpha = 0$ and $\alpha = 0.5$. The orientations of the a axes in two superconductor leads are set as $a_L = a_R = 0$ in panel (a), $a_L = a_R = \pi/4$ in panel (b), $a_L = 0$ and $a_R = \pi/4$ in panel (c). The other parameters are set as $T = 0.1T_c$, $L = 0.1\xi$, $\Delta_0 = 10^{-3}\mu$.

The numerical results shown above indicate that, due to the interplay of Rashba SOC and Zeeman splitting and d-wave pairing, anomalous Josephson current may occur at zero phase bias in the considered structure under various different situations, and both the magnitude and the direction of the anomalous Josephson current may depend sensitively not only on the relative orientations of the Zeeman field and the spin–orbit field in the bridge region but also on the relative orientations of the a axes in two superconductor leads. For example, the results shown in Fig. 1(b) and Fig. 2(b) indicate that if the a axes in two superconductor leads are parallel to each other, anomalous Josephson current may be induced by a Zeeman field orientating along the y axis in the bridge region. The results show in Figs. 3(a)– 3(c) indicate that if the a axes in two superconductor leads are misaligned, anomalous Josephson current may be induced by a Zeeman field orientating along an arbitrary direction in the bridge region. It also should be noted that, since both the first harmonics and the second harmonics may play important roles in the Josephson current in the considered structure and their relative weights may depend sensitively on a number of complicated factors, the anomalous Josephson effect in the considered structure can not be accounted for by simply introducing an anomalous phase shift in the CPR.

When the relative orientations of the Zeeman field and the spin–orbit field in the bridge region and the a axes in two superconductor leads are fixed, both the magnitude and the direction of the anomalous Josephson current may also depend sensitively on the strengths of the Zeeman field and the spin-orbit field in the bridge region. To illustrate this fact more clearly, in the following discussions we take the situations where the Zeeman field is orientated along the y axis as the examples. In Figs. 4(a)–4(c) we show the anomalous Josephson current I_a at zero phase bias as a function of the strength h_y of the Zeeman field for the Rashba SOC strength $\alpha = 0$ and $\alpha = 0.5$, with the orientations of the a axis in two superconductor leads set to be: (a) $a_L = a_R = 0$, (b) $a_L = a_R = \pi/4$, and (c) $a_L = 0$, $a_R = \pi/4$, respectively. Figures 4(a)–4(c) show that the anomalous Josephson current is suppressed obviously for $\alpha = 0$, independent of the strength h_y of the Zeeman field. In contrast, for $\alpha = 0.5$, a finite anomalous Josephson current may occur when $h_y \neq 0$. As the value of h_y is varied, the

anomalous Josephson current reverses its direction of flow frequently at approximately regular intervals and the magnitude of the anomalous Josephson current changes significantly in an oscillating manner, and the amplitude of the oscillations decreases gradually with the increase of h_y.

In Figs. 5(a)–5(c) we show the anomalous Josephson current I_a at zero phase bias as a function of the Rashba SOC strength α for the Zeeman field strength $h_y/\mu = 0$ and $h_y/\mu = 0.25$, with the orientations of the a-axis in two superconductor leads set along the same directions as in Figs. 4(a)–4(c), respectively. Figures 5(a)–5(c) show that, for $h_y/\mu = 0$, the anomalous Josephson current is suppressed obviously, independent of the Rashba SOC strength α. In contrast, for $h_y/\mu = 0.25$, a finite anomalous Josephson current may occur when α is sufficiently large. The anomalous Josephson current also changes in an oscillating manner as the value of α is varied, but unlike the results shown in Figs. 4(a)–4(c), both the amplitude and the period of the oscillations increase gradually with the increase of α.

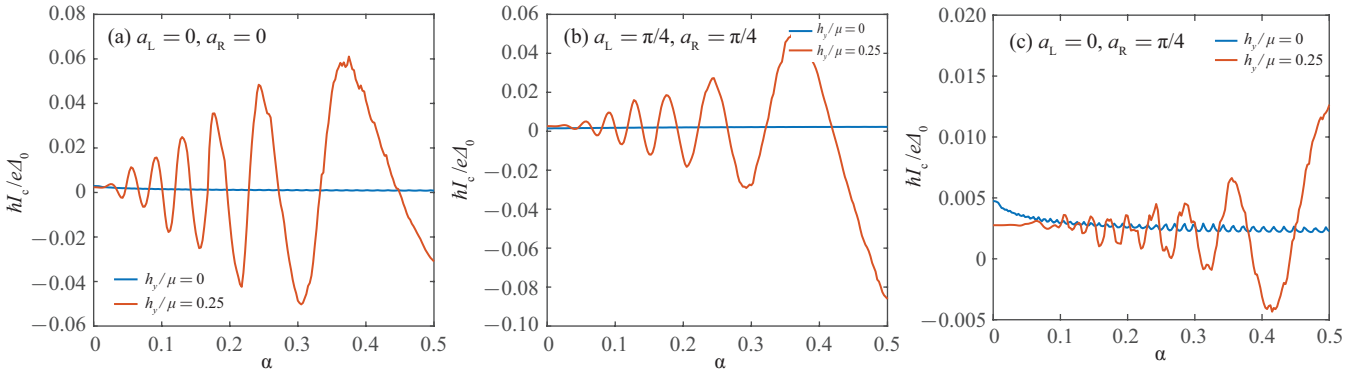


Fig. 5. The anomalous Josephson current I_a at zero phase bias as a function of the Rashba SOC strength α for the Zeeman field strength $h_y/\mu = 0$ and $h_y/\mu = 0.25$. The orientations of the a axes in two superconductor leads are set as $a_L = a_R = 0$ in panel (a), $a_L = a_R = \pi/4$ in panel (b), $a_L = 0$ and $a_R = \pi/4$ in panel (c). The other parameters are set as $T = 0.1T_c$, $L = 0.1\xi$, $\Delta_0 = 10^{-3}\mu$.

4. Conclusions

In summary, based on the Bogoliubov–de Gennes equation and the extended McMillan's Green's function formalism, we have presented a systematic theoretical investigation on the Josephson effect between two d-wave superconductors bridged by a ballistic 2DEG with both Rashba SOC and Zeeman splitting. The Josephson current and the CPR are calculated under various different situations. We show that due to the interplay of Rashba SOC and Zeeman splitting and d-wave pairing, the CPR in such a heterostructure may exhibit a series of novel features and can change significantly as some relevant parameters are tuned. In particular, anomalous Josephson current may occur at zero phase bias under various different situations when both time reversal symmetry and inversion symmetry of the system are simultaneously broken, which can be realized by tuning the relative orientations and the strengths of the Zeeman field and the spin–orbit field in the bridge region, the relative orientations of the a axes in two superconductor leads, or the relative orientations between the Zeeman field in the bridge region and the a axes in the superconductor leads. It is also shown that both the first and the second harmonics may play important roles in the Josephson current and their relative weights also depend sensitively on these complicated factors, and due to this fact, the anomalous Josephson current in the considered structure can not be accounted for by simply introducing an anomalous phase shift in the CPR.

References

[1] François Konschelle, Tokatly I V and Sebastián Bergeret F 2015 *Phys. Rev. B* **92** 125443
[2] Bujnowski B, Biele R and Bergeret F S 2019 *Phys. Rev. B* **100** 224518
[3] Maistrenko O, Scharf B, Manske D and Hankiewicz E M 2021 *Phys. Rev. B* **103** 054508
[4] Assouline A, Feuillet-Palma C, Bergeal N, Zhang T, Mottaghizadeh A, Zimmers A, Lhuillier E, Marangolo M, Eddrief M, Atkinson P, Aprili M and Aubin H 2019 *Nat. Commun.* **10** 126
[5] Gingrich E C, Niedzielski B M, Glick J A, Wang Y, Miller D L, Loloee R, Pratt W P Jr and Birge N O 2016 *Nat. Phys.* **12** 564
[6] Fu L and Kane C L 2008 *Phys. Rev. Lett.* **100** 096407
[7] Cayao J and Black-Schaffer A M 2017 *Phys. Rev. B* **96** 155426
[8] Feofanov A K, Oboznov V A, Bol'ginov V V, Lisenfeld J, Poletto S, Ryazanov V V, Rossolenko A N, Khabipov M, Balashov D, Zorin A B, Dmitriev P N, Koshelets V P and Ustinov A V 2010 *Nat. Phys.* **6** 593
[9] Baek B, Rippard W H, Benz S P, Russek S E and Dresselhaus P D 2014 *Nat. Commun.* **5** 3888
[10] Ortlepp T, Ariando, Mielke O, Verwijs C J M, Foo K F K, Rogalla H, Uhlmann F H and Hilgenkamp H 2006 *Science* **312** 1495
[11] Padurariu C and Nazarov Y V 2010 *Phys. Rev. B* **81** 144519
[12] Reynoso A A, Usaj G, Balseiro C A, Feinberg D and Avignon M 2012 *Phys. Rev. B* **86** 214519
[13] Kontos T, Aprili M, Lesueur J, Genêt F, Stephanidis B and Boursier R 2002 *Phys. Rev. Lett.* **89** 137007
[14] Halterman K, Valls O T and Wu C T 2015 *Phys. Rev. B* **92** 174516
[15] Dresselhaus G 1955 *Phys. Rev.* **100** 580
[16] Bychkov Y A and Rashba E I 1984 *J. Phys. C* **17** 6039
[17] Szombati D B, Nadj-Perge S, Car D, Plissard S R, Bakkers E P A M and Kouwenhoven L P 2016 *Nat. Phys.* **12** 568
[18] Edelstein V M 1990 *Solid State Commun.* **73** 233
[19] Meier L, Salis G, Shorubalko I, Gini E, Schön S and Ensslin K 2007 *Nat. Phys.* **3** 650
[20] Wilamowski Z, Malissa H, Schäffler F and Jantsch W 2007 *Phys. Rev. Lett.* **98** 187203
[21] Li C H, van't Erve O M J, Liu Y, Li L and Jonker B 2016 *Sci. Rep.* **6** 29533
[22] Shen K, Vignale G and Raimondi R 2014 *Phys. Rev. Lett.* **112** 096601

[23] Ganichev S, Ivchenko E, Belḱov V, Tarasenko S, Sollinger M, Weiss D, Wegscheider W and Prettl W 2002 *Nature* **417** 153

[24] Rojas Sánchez J C, Vila L, Desfonds G, Gambarelli S, Attané J P, De Teresa J M, Magén C and Fert A 2013 *Nat. Commun.* **4** 2944

[25] Bobkova I V, Bobkov A M, Zyuzin A A and Alidoust M 2016 *Phys. Rev. B* **94** 134506

[26] Bobkova I V and Bobkov A M 2017 *Phys. Rev. B* **95** 184518

[27] Costa A and Fabian J 2020 *Phys. Rev. B* **101** 104508

[28] Alidoust M 2020 *Phys. Rev. B* **101** 155123

[29] Alidoust M, Shen C and Žutić I I 2021 *Phys Rev B* **103** L060503

[30] Bezuglyi E V, Rozhavsky A S, Vagner I D and Wyder P 2002 *Phys. Rev. B* **66** 052508

[31] Buzdin A 2008 *Phys. Rev. Lett.* **101** 107005

[32] Houzet M, Meyer J S and Badiane D M 2013 *Phys. Rev. Lett.* **111** 046401

[33] Bèri B, Bardarson J H and Beenakker C W J 2008 *Phys. Rev. B* **77** 045311

[34] Zazunov A, Egger R, Jonckheere T and Martin T 2009 *Phys. Rev. Lett.* **103** 147004

[35] Liu J F and Chan K S 2010 *Phys. Rev. B* **82** 125305

[36] Mal'shukov A G, Sadjina A and Brataas A 2010 *Phys. Rev. B* **81** 060502

[37] Yokoyama T, Eto M and Nazarov Y V 2014 *Phys. Rev. B* **89** 195407

[38] Testa G, Sarnelli E, Monaco A, Esposito E, Ejrnaes M, Kang D J, Mennema S H, Tarte E J and Blamire M G 2005 *Phys. Rev. B* **71** 134520

[39] McMillan W L 1968 *Phys. Rev.* **175** 559

[40] Furusaki A and Tsukada M 1991 *Solid State Commun.* **78** 299

[41] Tanaka Y and Kashiwaya S 1997 *Phys. Rev. B* **56** 892

[42] de Gennes P G 1999 *Superconductivity of Metals and Alloys* (Westview Press, Reading, MA)

[43] Zhang W Y 1995 *Phys. Rev. B* **52** 3772

[44] Zhang W Y 1995 *Phys. Rev. B* **52** 12538

[45] Zhang W Y and Wang Z D 2002 *Phys. Rev. B* **65** 144527

[46] Lu B and Tanaka Y K 2018 *Philos. Trans. R. Soc. A* **376** 20150246